

β -detected NMR of Li in Ga_{1-x}Mn_xAs

Q. Song,¹ K. H. Chow,² Z. Salman,^{3,*} H. Saadaoui,^{1,*} M. D. Hossain,¹ R. F. Kiefl,^{1,3,4} G. D. Morris,³ C. D. P. Levy,³ M. R. Pearson,³ T. J. Parolin,⁵ I. Fan,² T. A. Keeler,¹ M. Smadella,¹ D. Wang,¹ K. M. Yu,⁶ X. Liu,⁷ J. K. Furdyna,⁷ and W. A. MacFarlane⁵

¹*Department of Physics and Astronomy, University of British Columbia, Vancouver, BC, Canada, V6T 1Z1*

²*Department of Physics, University of Alberta, Edmonton, AB, Canada, T6G 2G7*

³*TRIUMF, 4004 Wesbrook Mall, Vancouver, BC, Canada, V6T 2A3*

⁴*Canadian Institute for Advanced Research, Toronto, Ontario, Canada M5G 1Z8*

⁵*Chemistry Department, University of British Columbia, Vancouver, BC, Canada, V6T 1Z1*

⁶*Lawrence Berkeley National Laboratory, 1 Cyclotron Road, Berkeley, California 94720 USA*

⁷*Department of Physics, University of Notre Dame, Notre Dame, Indiana 46556 USA*

(Received 21 March 2011; published 5 August 2011; corrected 5 December 2011)

The magnetic properties of a 180-nm-thick epitaxial film of the dilute magnetic semiconductor Ga_{1-x}Mn_xAs with $x = 0.054$ are investigated using beta-detected NMR of low-energy implanted ⁸Li⁺. There is a broad distribution of local magnetic fields in the Ga_{1-x}Mn_xAs layer, reflecting the magnetic inhomogeneity of the system. The resonance (representing the local magnetic field distribution) is followed as a function of temperature through the ferromagnetic transition. The average hyperfine field at the ⁸Li nucleus is measured to be positive and on the order of 150 G at low temperature, implying a negative hyperfine coupling of the ⁸Li to the delocalized holes and suggesting that the holes are better described by an Mn-derived impurity band. The spin-lattice relaxation of ⁸Li shows a remarkably weak feature at the phase transition and no Korringa behavior despite metallic conductivity. No evidence is found of the microscopic magnetic phase separation that has been suggested by some low-energy muon spin-rotation measurements.

DOI: [10.1103/PhysRevB.84.054414](https://doi.org/10.1103/PhysRevB.84.054414)

PACS number(s): 76.60.-k, 74.62.Dh, 74.25.Ha

I. INTRODUCTION

It is widely accepted that ferromagnetism in the prototypical dilute magnetic semiconductor Ga_{1-x}Mn_xAs is driven by coupling between local Mn²⁺ $S = \frac{5}{2}$ moments mediated by delocalized holes.^{1,2} Detailed models of this mechanism involve parametrization of the relevant hole states, e.g. via the $k \cdot p$ approximation of the GaAs valence band (valence band model).³ However, at sufficiently high Mn concentration (divalent substitutional Mn on the Ga site is an electron acceptor), one should, instead, consider Mn impurity-derived hole states (impurity band model), and there is controversy over which is the appropriate picture for the highest magnetic transition temperature (T_C) compositions well into the metallic conduction regime.^{4,5} Optical,⁶ transport,⁷ and recent scanning tunneling microscopy⁸ (STM) results favor the impurity band model, while a variety of features are consistent with the valence band model.^{2,9} Calculations predict that in the ferromagnetic ground state the hole magnetization is opposite to (and much weaker than) that of the Mn local moments.¹ The delocalized holes play a crucial role in the formation of the magnetic ground state; however, little is known experimentally about their magnetization and its variation with temperature. Macroscopic magnetometry can only measure the total magnetic moment and cannot easily distinguish various contributions, so it cannot provide such information. Spectroscopically resolved magneto-optical measurements^{10,11} are sensitive to the mobile holes, but careful modeling is required to extract their magnetization. Such measurements, like bulk magnetometry, report the net behavior over a macroscopic region of the sample and yield no information on the microscopic magnetic inhomogeneity. Tunneling spectroscopy in magnetic tunnel junctions can also measure the spin polarization at the Fermi level,^{4,12,13} and spatially

resolved STM can, in principle, measure its inhomogeneity. However, such measurements reflect the behavior very near the surface or interface and may not be representative of the bulk. It is thus important to pursue other complementary means to elucidate the magnetic properties of the itinerant holes. In this context, nuclear magnetic resonance (NMR) is an atomically resolved magnetic probe that senses the average hole contribution through a shift of the resonance, analogous to the Knight shift in a paramagnetic metal.¹⁴ As the material is intrinsically inhomogeneous, an atomically resolved probe also reveals the associated magnetic inhomogeneity, through broadening and structure of the resonance line, for example, in the controversial proposal of magnetic phase separation.¹⁵⁻¹⁷ Nuclear spin lattice relaxation yields information on the low frequency spin dynamics where correlations are expected to play an important role.¹⁸

The equilibrium solubility limit of Mn in GaAs is very low, so the production of Ga_{1-x}Mn_xAs at the high Mn concentrations necessary for ferromagnetism requires nonequilibrium growth in the form of thin films, and bulk samples are not available. Because of signal limitations, NMR cannot generally be used for thin films, but when NMR is detected by the anisotropy of radioactive β -decay (for a *beta*-radioactive NMR nucleus), it is possible to overcome this limitation. In this paper, we use an implanted hyperpolarized beam of ⁸Li⁺ to study a thin film of Ga_{1-x}Mn_xAs using β -NMR. We present both resonance and spin lattice relaxation data as a function of temperature in a 180-nm-thick epitaxial film of Ga_{1-x}Mn_xAs with $x = 0.054$. Only in a few cases has β -NMR been carried out in a ferromagnet.^{19,20} Since this is the first example in a disordered ferromagnet, it was not clear, prior to the experiment, whether the ⁸Li⁺ spin relaxation would be slow enough, or the resonance narrow enough, to follow through the transition; however, the signals are clearly observable, and the

results afford a novel local-probe view of the magnetic state in this important dilute ferromagnet.

First, we review what is known about the β -NMR of $^8\text{Li}^+$ implanted in semi-insulating GaAs. The absence of quadrupolar splitting of the resonance implies $^8\text{Li}^+$ occupies a cubic site, likely the arsenic tetrahedral interstitial. This site appears stable up to about 200 K, above which there is evidence of a site change to another cubic site; however, the resonance position does not change substantially below 300 K.^{21,22} The line width of the resonance is about 3 kHz, consistent with nuclear dipolar broadening by the surrounding Ga and As nuclear moments. This implies $^8\text{Li}^+$ contributing to the resonance are not near any Frenkel (vacancy, interstitial) pairs created by the implantation. Broad lines corresponding to noncubic sites near implantation damage may occur, particularly at low temperature, e.g., as seen for ^{12}B implantation in ZnSe,²³ but they do not contribute to the resonances reported here.

One of the major advantages of β -NMR using a low-energy ion beam is the possibility to vary the implantation energy by electrostatic deceleration and thus probe the sample as a function of depth. We now briefly summarize a preliminary work (Ref. 24) that reported such a depth-dependent study in the current $\text{Ga}_{1-x}\text{Mn}_x\text{As}$ sample at 50 K. The observed spectrum consists of two lines, one narrow (width consistent with pure GaAs) and one much broader and centered at a lower frequency. The systematic dependence of this composite spectrum on implantation energy indicates that the broad line is associated with the Mn-doped overlayer, while the narrow line is associated with the GaAs substrate. Quantitative comparison with Monte Carlo predictions of the implantation profile, however, reveals that the narrow line persists to unexpectedly low implantation energies. We suspect this is the result of implantation channelling²⁵ that is not accounted for in the simulation. The spin relaxation also varied systematically with implantation energy with fast relaxation associated with the magnetic overlayer and much slower relaxation with the substrate. In the current work, we implant the $^8\text{Li}^+$ beam at 8 keV. At this energy, the spectrum contains both the narrow and broad resonances. The substrate resonance provides a convenient *in situ* calibration of the applied magnetic field.

II. EXPERIMENTAL

The β -NMR experiment was carried out at the isotope separator and accelerator (ISAC) facility at TRIUMF using a beam of highly polarized radioactive $^8\text{Li}^+$ with a typical flux of $\sim 10^6/s$ into a beam spot about 3 mm in diameter centered on the sample. The ^8Li nucleus has spin 2, lifetime $\tau = 1.21\text{s}$, gyromagnetic ratio $\gamma = 630.15\text{ Hz/G}$, and an electric quadrupole moment $Q = +31.4\text{ mb}$. Details of the polarizer and spectrometer can be found in Refs. 26 and 27. The $^8\text{Li}^+$ beam is decelerated from 28 to 8 keV immediately prior to implantation into the sample. Simulation of the implantation profile indicates an average depth of 46 nm at this energy, with a half-width of 24 nm. Resonance measurements are carried out with a continuous beam in a static magnetic field $H_0 = 1.33\text{ T}$. To measure the spin-lattice relaxation rate T_1 , the ion beam is pulsed with an electrostatic kicker and the time dependence of the β -decay asymmetry is monitored during and after each pulse. The beam pulse was on for 4 s and then off for a counting

period of 12 s. Decay events were accumulated by repeating this cycle for ~ 30 minutes per temperature.

Because of the sensitivity of the β -detection, relatively few ions are required for the measurement. The total implanted fluence of $^8\text{Li}^+$ (in ~ 4 days of measurement) was on the order of $10^{12}/\text{cm}^2$. Comparison with the effects of much higher energy ions indicates we can expect little or no net effect of the implantation on the macroscopic properties of the sample.²⁸ This is confirmed by the fact that we found no time dependence in the results over the course of the experiment and between runs on the same sample.²⁹

We present data on a 180-nm $\text{Ga}_{1-x}\text{Mn}_x\text{As}$ film grown on a $8.5 \times 6.5\text{-mm}$ semi-insulating (100) GaAs single-crystal substrate in a Riber 32 R&D molecular beam epitaxy system and subsequently annealed at 280°C for 1 hour. More information on the epitaxial growth can be found elsewhere.³⁰ Low-field SQUID magnetometry was used to determine $T_C = 72\text{ K}$, and the Mn site occupancies were determined by c-PIXE and c-RBS to be 74.5% of Mn at Ga substitutional sites, 21.5% Arsenic interstitial sites, and 4% in nonspecific “random” sites.³¹ Transport measurements indicate this film is metallic with low-temperature resistivity $\sim 30\text{ m}\Omega\text{-cm}$.

III. RESONANCE SPECTRA

The resonance spectra of $^8\text{Li}^+$ at 8 keV implantation energy and 1.33 Tesla are shown for various temperatures in Fig. 1. At 50 K, the spectrum is similar to that reported in Ref. 24, with both broad (overlayer) and narrow (substrate) resonances. There is no evidence of quadrupolar splittings in any of the spectra,³² consistent with the cubic $^8\text{Li}^+$ sites known in GaAs. For the broad line, this is somewhat surprising, since the heterovalent Mn dopants must locally break cubic symmetry. Cubic symmetry will be restored upon averaging over all sites, but a distribution of unresolved quadrupolar interactions may contribute to the width of the resonance. ^8Li that stop in sites immediately adjacent to Mn will experience the largest electric field gradients and hence the largest quadrupolar splittings. However, such ^8Li will also experience such strong local magnetic fields and fast spin relaxation that they will not likely contribute to the observed resonance. In fact, the occurrence of Mn–Li defect complexes in GaAs was studied long ago by Mn EPR.³³

At the highest temperature, the two resonances are unresolved, and there is little evidence of the broad peak. But as T is reduced, the broad line shifts out of the narrow resonance and broadens continuously, becoming too broad to observe with the limited radio frequency (rf) magnetic field of the broadband spectrometer (amplitude, $H_1 \leq 100\mu\text{T}$) below about 30 K. In dilute magnetic alloys, the lineshape is expected to be approximately Lorentzian, though for concentrations at the level of a few %, there are some deviations.³⁴ The pseudo-Lorentzian lineshape is the result of a broad distribution of distances between probe nuclei and the nearest local magnetic moment combined with the power law decay of the magnetic field away from the local moments. We fit the data to the sum of two Lorentzians (curves in Fig. 1),

$$A(\nu) = \frac{A_{\text{sub}}\sigma_{\text{sub}}^2}{4(\nu - \nu_{\text{sub}})^2 + \sigma_{\text{sub}}^2} + \frac{A_{\text{mag}}\sigma_{\text{mag}}^2}{4(\nu - \nu_{\text{mag}})^2 + \sigma_{\text{mag}}^2} \quad (1)$$

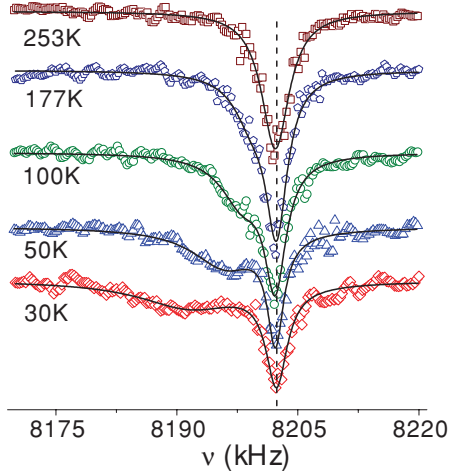


FIG. 1. (Color online) Temperature dependence of the β -NMR spectra (vertically offset for clarity) of $^8\text{Li}^+$ in $\text{Ga}_{1-x}\text{Mn}_x\text{As}$ with implantation energy 8 keV. ^8Li in the substrate produces the narrow resonance while the broad resonance originates in the $\text{Ga}_{1-x}\text{Mn}_x\text{As}$ overlayer.

where ν_i, σ_i , and A_i are the resonance positions, widths (FWHM), and amplitudes, with $i = \text{mag}$ and sub denoting the broad line in the overlayer and the narrow substrate resonance, respectively. The position of the substrate resonance ν_{sub} was constrained to be independent of temperature, consistent with measurements in pure GaAs.²² Above 250 K and below 30 K, the two lines are unresolved, so a single Lorentzian was used. Lorentzian fits were adequate but were only significantly better than Gaussian fits in the high temperature region above 200 K.

The results of this analysis are summarized in Fig. 2. As is evident in the raw data (Fig. 1), the broad line shifts toward lower frequency and broadens as temperature is reduced. Measurements at other fields (not shown) indicate the shift is magnetic in origin, scaling linearly with field. The slight temperature dependence of the amplitude of the substrate line A_{sub} , is consistent with previous measurements in pure GaAs.²² It may be due to ^8Li stopping in noncubic sites produced by implantation-related damage, e.g., arsenic vacancies, as has been observed for ^{12}B implantation in ZnSe.²³ The amplitude of the broad resonance A_{mag} decreases as the line broadens, as expected for a constant applied rf field. There is no evidence of a sharp change of either amplitude through T_C , nor is there a sharp change of the total area of the spectrum at T_C . Continuity of the amplitude through T_C is in contrast to the conventional NMR “wipeout effect” that often accompanies such a transition.³⁵

Using the substrate frequency, we measure the average internal field sensed by the ^8Li in the Mn-doped layer, B_{int} by the raw shift of the resonance $\Delta\nu$:

$$\Delta\nu = \nu_{\text{mag}} - \nu_{\text{sub}} = \gamma \Delta B, \quad (2)$$

with $\Delta B = B_{\text{int}} - B_0$ and B_0 the applied external field. We discuss the various contributions to B_{int} in Section V below.

We now turn to the width of the overlayer resonance. Though the linewidths are from Lorentzian fits, we decompose different contributions assuming all other broadening mechanisms add in quadrature to the GaAs width,³⁴ i.e.,

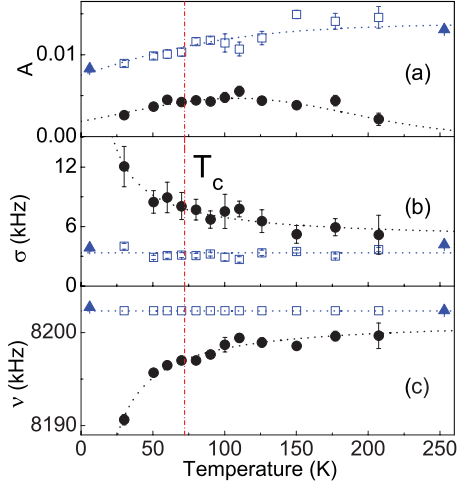


FIG. 2. (Color online) The amplitude A , linewidth σ , and position ν as a function of temperature from Lorentzian fits to the resonance spectra of ^8Li implanted at 8 keV in an applied field of 1.33 T. The open squares refer to the narrow substrate resonance, the closed circles to the broad line from the Mn-doped layer, and the filled triangles to single Lorentzian fits. The width and position of the substrate line do not change substantially with temperature, in contrast to the resonance from the magnetic layer. The broken vertical line indicates T_C .

$\sigma_{\text{mag}}^2 = \sigma_{\text{sub}}^2 + \sigma_{\text{Mn}}^2$, where σ_{Mn} represents the additional broadening due to Mn doping. As shown in Fig. 2(b), σ_{sub} is approximately constant below 200K, therefore the increase in σ_{mag} at low temperature is due to the Mn doping. As the shift of the broad line represents the average total field in the $\text{Ga}_{1-x}\text{Mn}_x\text{As}$ layer, the broadening represents a distribution of this field; however, there can be other nonmagnetic sources of broadening. In particular, as ^8Li is quadrupolar, the width is sensitive to a distribution of electric field gradients caused by the static charge disorder produced by ionized Mn acceptors. The assumption that the quadrupolar (σ_q) and magnetic broadening (σ_M) also add in quadrature: $\sigma_{\text{Mn}}^2 = \sigma_q^2 + \sigma_M^2$ achieves a good fit (see Section V). σ_q is expected to be independent of T when $^8\text{Li}^+$ is not mobile, as is the case below room temperature.

IV. SPIN-LATTICE RELAXATION

In order to better understand the resonance data and to probe the magnetic dynamics in $\text{Ga}_{1-x}\text{Mn}_x\text{As}$, we performed spin lattice relaxation experiments under the same conditions as the resonances presented above. As expected from the two line spectra, we find a two component relaxation of the ^8Li nuclear spin polarization. At 8 keV implantation energy, we find a small almost nonrelaxing component, consistent with slow relaxation in the GaAs substrate, and a large, much faster relaxing component from the $\text{Ga}_{1-x}\text{Mn}_x\text{As}$. The implantation energy dependence of the relaxation confirms these assignments.²⁴ We fit the relaxation assuming a simple biexponential form for the polarization p at time t after implantation:

$$p(t) = A_{\text{mag}} e^{-\lambda_{\text{mag}} t} + A_{\text{sub}} e^{-\lambda_{\text{sub}} t}, \quad (3)$$

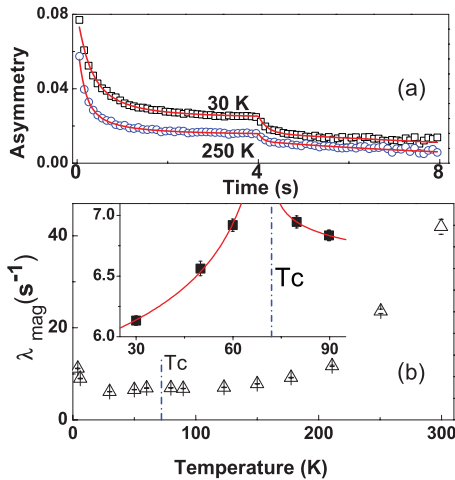


FIG. 3. (Color online) (a) Time dependence of the average $^8\text{Li}^+$ spin polarization during and after the beam pulse at 30 K (below T_C) and at 250 K (above T_C) at 8 keV beam energy in the field of 1.33 T. The relaxation rate is faster at 250 K than at 30 K. (b) The spin-lattice relaxation rate λ_{mag} in the overlayer as a function of temperature. The increase in λ_{mag} above 150 K is consistent with an increase in pure GaAs³⁷ and may be due to the onset of the $^8\text{Li}^+$ site change. Inset: An enlarged plot showing a slight enhancement of λ_{mag} in the vicinity of T_C , in contrast to the divergence expected from critical slowing down of spin fluctuations at the transition.

where A_i is the initial amplitude for each component, and $\lambda_i = 1/T_1^i$ the corresponding relaxation rate. We fit the experimental data to the convolution of $p(t)$ with the beam pulse to extract the relaxation rate $\lambda_{\text{mag}}(T)$ at 1.33 Tesla.³⁶ Examples of the fits are shown in Fig. 3(a). In these measurements, the beam is on continuously until 4 s, when it is turned off, yielding the sharp change at this time. While the beam is on, the measured asymmetry approaches a dynamic equilibrium value determined by the rate of spin relaxation and the radioactive lifetime τ of the $^8\text{Li}^+$ probe. That the 250 K relaxation spectrum lies consistently below the 30 K data is direct evidence that the relaxation is faster at 250 K. The data shown do not appear to have the same total amplitude, likely because there is some very fast relaxation at 250 K which is not captured with the experimental time resolution. Though the fits are reasonably good, this behavior may indicate that the relaxation is not a simple exponential as in Eq. (3). In fact, in an inhomogeneous system, one expects a distribution of relaxation rates corresponding to the distribution of static fields evidenced by the line broadening. Since the polarization of ^8Li in the beam is constant, we fixed the amplitudes in the fits, accounting for the full variation in temperature with only the relaxation rates. Thus λ_{mag} extracted from the fits represents an average relaxation rate for ^8Li in the $\text{Ga}_{1-x}\text{Mn}_x\text{As}$ layer. While λ_{sub} varies with T , it remains much smaller than λ_{mag} for all temperatures.

The temperature dependence of λ_{mag} is shown in Fig. 3(b). The most obvious feature is the substantial increase in λ_{mag} above 200 K. Such an increase is unexpected for a simple paramagnet, which, naively, should exhibit a monotonic decrease of the spin relaxation rate above T_C as spin fluctuations become progressively faster with increasing temperature. The increase, however, may be related to a similar increase³⁷

found in pure GaAs that is thought to be due to the $^8\text{Li}^+$ site change.^{21,22} Enhanced relaxation could result from a stronger hyperfine coupling in the high-temperature site, or, if the site change is due to the onset of interstitial $^8\text{Li}^+$ diffusion, to the formation of Mn–Li defect complexes.³³ The high temperature increase of λ_{mag} accounts in part for the disappearance of the broad resonance at higher temperature. λ_{mag} also increases at the lowest temperature, in contrast to the behavior of a homogeneous ferromagnet. This may be due to some Mn spins remaining paramagnetic well below T_C making a Curie-law contribution to λ_{mag} . Between these limits, λ_{mag} is relatively constant but exhibits a slight peak near T_C [inset of Fig. 3(b)], where critical slowing down of the Mn moments should yield a divergence in the relaxation rate.³⁸ While the critical region is broadened by the applied field, as well as the microscopic inhomogeneity of the alloy, e.g., as in $\text{La}_{0.67}\text{Ca}_{0.33}\text{MnO}_3$,³⁶ the relatively weak temperature dependence through T_C is still surprising. The magnitude of λ_{mag} is large, not only much larger than in undoped GaAs, but also ~ 10 times the rate in metallic Ag, consistent with it originating in the magnetism of $\text{Ga}_{1-x}\text{Mn}_x\text{As}$. In general, λ is a measure of the spectral density of (transverse) magnetic fluctuations at the NMR frequency. The absence of a peak suggests that the spin dynamics that dominates the $^8\text{Li}^+$ relaxation does not change dramatically through the formation of a static moment, in contrast to homogeneous metallic³⁸ or semiconducting³⁹ ferromagnets. Neither does λ follow the linear (Korringa) temperature-dependence characteristic of metals^{40,41} that might be anticipated if the relaxation was predominantly due to interaction with a degenerate fluid of delocalized holes in this metallic alloy. However, it is similar to what is found in doped nonmagnetic semiconductors when the Fermi level lies in a narrow impurity band.⁴²

V. ANALYSIS AND DISCUSSION

We now extend the analysis on the results presented above beginning with the resonance shift. The difference in the average magnetic field between the overlayer and the substrate ΔB is due to the Mn doping, so we decompose the internal field into various contributions from the surrounding magnetized layer and the applied field B_0 ,

$$B_{\text{int}} = B_0 + B_{\text{demag}} + B_{\text{Lor}} + B_{\text{loc}}, \quad (4)$$

assuming for simplicity that all contributions are parallel at high applied fields. Here, B_{demag} is the demagnetization field determined by the macroscopic shape of the sample, B_{Lor} is the field due to the Lorentz cavity that divides the sample into a local region that must be treated atomically from the rest of the sample, which may be treated as a homogeneous magnetic continuum, and B_{loc} is the local field from the atomic environment within the Lorentz cavity, including the contact hyperfine interaction between mobile holes and the probe nucleus that gives rise, for example, to the Knight shift in metals.⁴³ It is B_{loc} that is of interest as a measure of the polarization of the delocalized holes.

At the Mn concentration of this sample, there is about one Mn ion per 5 GaAs unit cells (cubic lattice constant $\sim 5.7 \text{ \AA}$ ⁴⁴) so there is no difficulty defining a Lorentz cavity much smaller than the film thickness outside of which the $\text{Ga}_{1-x}\text{Mn}_x\text{As}$ can

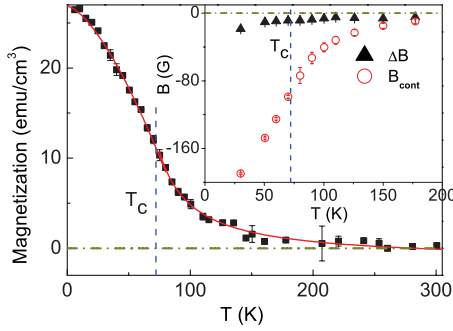


FIG. 4. (Color online) The temperature dependence of volume magnetization M at 1.33 T field. The magnitude of $M(T \rightarrow 0)$ is on the order expected for full polarization of the Mn local moments for the known Mn concentration and thickness. The inset shows a comparison of $\Delta B = B_{\text{int}} - B_0$ (solid black triangles) and the continuum internal field $B_{\text{cont}} = -\frac{8}{3}\pi M$ (open red circles). The difference of these indicates that the local field is substantial and nearly cancels B_{cont} .

be treated as a continuum. To an excellent approximation, a thin film of uniform thickness in a perpendicular magnetic field has the maximal demagnetizing field, $B_{\text{demag}} = -4\pi M$ (cgs), where M is the continuum magnetization, while for a spherical Lorentz cavity,⁴³ $B_{\text{Lor}} = (4\pi/3)M$. In order to account for these contributions, we need a measure of M . To this end, we carried out SQUID magnetometry on a small piece of the sample at the same applied field. The resulting magnetic moment was then corrected for substrate and sample holder contributions and converted to the average volume magnetization using the nominal film thickness. The resulting $M(T)$ is shown in Fig. 4. Using this M , the continuum contribution to the internal field is $B_{\text{cont}} = B_{\text{demag}} + B_{\text{Lor}}$, which is plotted in the inset of Fig. 4 together with the measured ΔB for comparison. In using the substrate frequency as a measure of B_0 , we have neglected any chemical shift of the ^8Li in GaAs. The chemical shift is likely very small, consistent with the resonance position being very close to that in the cubic insulator MgO, our standard reference material.⁴⁵ We have also assumed that M is not contaminated by contributions from nonuniformity of the sample, such as impurity phases, e.g., occurring at either the surface of the film or at the interface with the substrate. This is reasonable as the measured M is consistent with the literature for films of this composition.⁴⁶

From Eq. (4),

$$B_{\text{loc}} = \Delta B - B_{\text{cont}},$$

so that the small observed value of ΔB implies B_{loc} must oppose and nearly cancel B_{cont} , i.e., at low temperature B_{loc} is on the order of +150 G. We use the above to calculate $B_{\text{loc}}(T)$ and plot it as a function of $M(T)$ in Fig. 5, together with the shift ΔB and linewidth σ_{Mn} . The clear correlation between B_{loc} and M is embodied in the linear fit $B_{\text{loc}} = (7.78 \pm 0.09) \times M[\text{G}] - (3 \pm 1)$ shown in Fig. 5(a). This linearity is not surprising, since B_{loc} is calculated with a large continuum contribution proportional to M . The ^8Li site is cubic on average, so only isotropic contributions to the average B_{loc} will be nonzero.⁴⁷ Such fields arise from the contact hyperfine interaction, here due to a mixing of the unoccupied

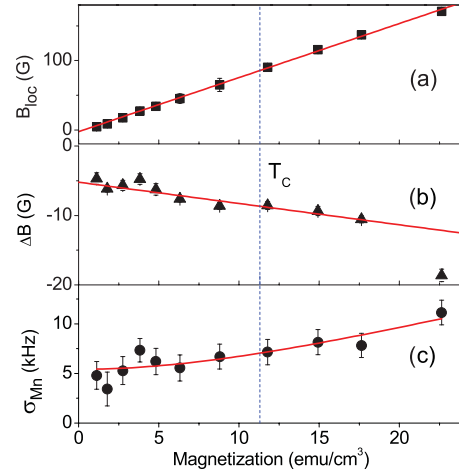


FIG. 5. (Color online) (a) The local field B_{loc} after demagnetization correction as a function of the volume magnetization M . The vertical intercept appears slightly different from zero. This is likely due to a slight uncertainty in the background correction for the SQUID measurement of M . (b) The raw field shift ΔB as a function of volume magnetization M . The nonlinearity at low temperature indicates B_{loc} is not simply proportional to the measured bulk magnetization. (c) The excess linewidth σ_{Mn} as a function of M fit to Eq. (6). The temperature independent quadrupolar broadening σ_q is found to be 5.6 ± 0.4 kHz.

^8Li 2s orbital with partly occupied electronic states of the surroundings, principally the delocalized holes. In this case, B_{loc} should scale with the hole magnetization, M_h , rather than the full magnetization M , i.e.,

$$B_{\text{loc}} = \left(\frac{A}{N_A \mu_B} \right) M_h, \quad (5)$$

where N_A is the Avogadro's number, μ_B is the Bohr magneton, and A is the hyperfine coupling constant. In paramagnetic metals, this is usually stated as $B_{\text{loc}} \propto \chi$, the spin susceptibility of the conduction band. Instead, we express B_{loc} in terms of the field-cooled M to avoid the nonlinearity (hysteresis) in $M(H)$ below T_C . The total macroscopic $M = M_h + M_{\text{Mn}}$, where the dominant term is M_{Mn} the magnetization due to the Mn^{2+} local moments, and M_h is predicted to be negative and much smaller on the order of a few percent of M .⁴⁸ While we have no independent measure of M_h , the strong coupling between the holes and Mn moments suggests that $M_h(T)$ should follow the temperature dependence of $M(T)$. Assuming M_h is $\approx 1\%$ of M , as theory suggests,¹ the coupling $A = -160 \pm 2 \text{ kG}/\mu_B$ is much stronger than in metals such as Ag ($20.6 \text{ kG}/\mu_B$).^{27,49} While B_{loc} is evidently positive, M_h is predicted to be negative,⁴⁸ so A is also negative. Negative A is unexpected from a simple picture where it is due to hybridization of the Li 2s orbital with the surrounding GaAs derived valence band. Li is also not likely to exhibit negative A from ‘‘core polarization.’’⁵⁰ For $^8\text{Li}^+$ negative A does, however, have precedent in some transition metals where the Fermi level falls in the d band (Pd [Ref. 40], Pt [Ref. 51] as well as ferromagnetic Ni [Ref. 19]). Here, a negative s - d coupling arises from the d band wavefunction's behavior at the interstitial position.^{52,53} In $\text{Ga}_{1-x}\text{Mn}_x\text{As}$ negative A may

similarly originate in the Mn-derived impurity band picture, where the holes have Mn *d* orbital character. However, detailed calculations for interstitial Li⁺ in both pure and doped GaAs would be necessary to put such a conclusion on a firm footing.

A more stringent test of whether $M_h(T)$ is simply proportional to $M(T)$ comes from considering the raw field shift ΔB , which represents the balance between two nearly canceling terms, the continuum field that certainly scales with the average $M(T)$ and B_{loc} , which may have a different T dependence. In Fig. 5(b), ΔB is plotted versus M , demonstrating a linear relationship $(-0.31 \pm 0.03) \times M - (5.2 \pm 0.3)$ that persists through T_C but breaks down at the lowest temperature (30 K), indicating that well into the ferromagnetic state the role of the delocalized holes is changing, possibly as temperature falls into the range of the impurity bandwidth. Alternatively, this deviation could be related to the onset of superparamagnetic effects seen in field-effect heterostructures,¹⁷ which may also lead to the observed increase in the spin relaxation at low T (Fig. 3).

We now consider the temperature dependence of the linewidth. Assuming the broadening of the resonance in the Ga_{1-x}Mn_xAs layer is a combination of a temperature-independent quadrupolar broadening (σ_q) from charge disorder and a magnetic broadening that scales with magnetization ($\sigma_m = \alpha M$):

$$\sigma_{Mn}^2 = \sigma_q^2 + (\alpha M)^2. \quad (6)$$

We fit σ_{Mn} to Eq. (6) as shown in Fig. 5(c) and find the quadrupolar broadening σ_q is 5.6 ± 0.4 kHz and $\alpha = 0.43 \pm 0.04$ kHz/(emu/cm³). Due to the randomly located Mn²⁺ local moments, we expect a distribution in the local magnetic field at the ⁸Li site that will thus give rise to an inhomogeneous broadening of the line that scales with M_{Mn} (or practically with M). Such a broadening is well established in the NMR of dilute magnetic alloys.⁵⁴ The observed width indicates the local magnetic field distribution is relatively broad in the sense that its width is comparable to its average (the shift), e.g., at the highest M (lowest T), σ_m at the highest magnetization is ~ 9.4 kHz (corresponding to ~ 15 G), comparable to the shift ΔB in Fig. 5(b). Using the dilute limit result of Ref. 34, we quantitatively estimate the broadening due to the Mn_{Ga} dipolar fields, neglecting interstitial Mn and any inhomogeneous polarization of the mobile holes (RKKY oscillations). Assuming $M \approx M_{Mn}$, we estimate the linewidth to be ~ 22.3 kHz at 30 K. Alternatively, this yields an estimate for the parameter $\alpha = 1.02$ for coupling to M of the substitutional Mn, substantially larger than the fit value in Fig. 5(c). This discrepancy is likely a consequence of the relatively high concentration, where the dilute limit expression overestimates the broadening, and the magnetic compensating effect of the interstitial Mn.¹ Note that neutron reflectometry has shown there may be a gradient in the interstitial Mn concentration through the film.⁵⁵ Such a gradient may thus cause a depth dependence of the ⁸Li resonance and will be the subject of a future study.

We now return to the question of phase separation. Some low energy μ SR (LE μ SR) experiments¹⁵ find that the ferromagnetic state is nanoscopically separated into comparable volumes of ferromagnetic and paramagnetic phases. In

contrast, also using LE μ SR, Dunsiger *et al.* find no evidence for phase separation in their samples.¹⁶ In our data, the single broad resonance in the overlayer shows no indication of this inhomogeneity below T_C , but unlike LE μ SR, we lack an absolute calibration of the resonance amplitude (which depends on the details of the applied rf pulses). Therefore, from the data of Fig. 1, we cannot put a quantitative limit on the existence of other phases. One might consider whether the observed narrow substrate resonance also contains a signal from ⁸Li in regions of the overlayer that remain paramagnetic. This is not supported by the implantation depth dependence, which shows this signal disappears at lower implantation energies.²⁴ Nanoscopic paramagnetic regions within the Mn-doped layer would also experience the same large continuum field B_{cont} and would shift with temperature, in contrast to the narrow resonance in Fig. 1. If, on the other hand, either of the two phase separated regions was unobserved in our spectra, e.g., if the spin relaxation was very fast or the static internal field was so large that the resonance occurred outside our frequency range, we would expect to lose some resonance *amplitude* at the transition; however, the continuous change of both amplitudes [Fig. 1(c)], and the integrated area of the resonance through T_C does not support this.

Using resonance data collected in a continuous wave rf mode (not shown), we have sufficient rf power to fully saturate the resonance at room temperature,⁵⁶ while at lower temperature, the line is too broad to saturate. Using the integral of the room temperature spectrum as a calibration of the full amplitude corresponding to all the ⁸Li, we find that the integrated spectrum (which accounts for the broadening) at 100 K corresponds to 73% of the room temperature value, and at 60 K to about 62%. Thus, through the transition, the loss of signal corresponds to only about 11% of the ⁸Li, much smaller than found by LE μ SR.¹⁵ We recall the amplitude in pure GaAs also depends on temperature [Fig. 2(a)], and this may account for much or all of the amplitude change here. The lack of evidence for phase separation may be a consequence of differences in the samples used in Ref. 15, which differed both in Mn concentration and in T_C . In contrast, our results are consistent with the full volume fraction magnetism found by a “wipeout effect” of the weak transverse field LE μ SR in samples with a range of Mn concentrations encompassing that of the current sample.¹⁶

VI. CONCLUSIONS

We have studied the magnetic properties of an epitaxially grown Ga_{1-x}Mn_xAs thin film, a dilute ferromagnetic semiconductor, with low energy implanted ⁸Li⁺, a β -NMR local magnetic probe. Since this is the first report on the temperature dependence of β -NMR resonances through T_C in a ferromagnet, it will be an important reference point to compare with other ferromagnets.

We clearly resolve resonances from both the nonmagnetic GaAs substrate and surprisingly from the magnetic film. The temperature dependence of the resonance position in the film indicates that the hole contribution to the magnetization scales with the macroscopic magnetization through T_C but then deviates below ~ 40 K. The hyperfine coupling constant of ⁸Li⁺ in Ga_{1-x}Mn_xAs is unexpectedly found to be negative,

which may indicate the Fermi level falls into a Mn-derived impurity band. There is no evidence for magnetic phase separation below T_C . The spin relaxation rate shows a small enhancement at T_C and no sign of the Korringa behavior that might be expected for this metallic alloy. Combined with these results, reliable *ab initio* calculations of the hyperfine coupling of $^8\text{Li}^+$ to the valence band of GaAs (and the Mn derived impurity band) may distinguish the appropriate microscopic model for the delocalized holes. A more complete picture will be obtained from a systematic study of $\text{Ga}_{1-x}\text{Mn}_x\text{As}$ as a function of Mn concentration, which could also include

the effects of film thickness, field-effects and optical carrier excitation.

ACKNOWLEDGMENTS

This research is supported by the Centre of Materials and Molecular Research at TRIUMF, the Natural Science and Engineering Research Council of Canada (NSERC), and Canadian Institute for Advanced Research (CIFAR) and National Science Foundation (US) Grant No. DMR06-03762. We thank M. Berciu for useful discussions.

*Present address: Laboratory for Muon Spin Spectroscopy, Paul Scherrer Institut, CH-5232 Villigen PSI, Switzerland.

¹T. Jungwirth, J. Sinova, J. Masek, J. Kucera, and A. H. MacDonald, *Rev. Mod. Phys.* **78**, 809 (2006).

²T. Dietl, H. Ohno, F. Matsukura, J. Cibert, and D. Ferrand, *Science* **287**, 1019 (2000); T. Dietl, H. Ohno, and F. Matsukura, *Phys. Rev. B* **63**, 195205 (2001).

³For example, E. O. Kane in *Handbook on Semiconductors*, T. S. Moss, ed. (North-Holland, Amsterdam, 1982), Vol. 1, Chap. 4A, p. 193.

⁴S. Ohya, I. Muneta, P. N. Hai, and M. Tanaka, *Phys. Rev. Lett.* **104**, 167204 (2010).

⁵F. Popescu, C. Sen, E. Dagotto, and A. Moreo, *Phys. Rev. B* **76**, 085206 (2007).

⁶K. Ando, H. Saito, K. C. Agarwal, M. C. Debnath, and V. Zayets, *Phys. Rev. Lett.* **100**, 067204 (2008); K. Hirakawa, S. Katsumoto, T. Hayashi, Y. Hashimoto, and Y. Iye, *Phys. Rev. B* **65**, 193312 (2002); V. F. Sapega, M. Moreno, M. Ramsteiner, L. Däweritz, and K. H. Ploog, *Phys. Rev. Lett.* **94**, 137401 (2005); K. S. Burch, D. B. Shrekenhamer, E. J. Singley, J. Stephens, B. L. Sheu, R. K. Kawakami, P. Schiffer, N. Samarth, D. D. Awschalom, and D. N. Basov, *ibid.* **97**, 087208 (2006).

⁷K. Alberi, K. M. Yu, P. R. Stone, O. D. Dubon, W. Walukiewicz, T. Wojtowicz, X. Liu, and J. K. Furdyna, *Phys. Rev. B* **78**, 075201 (2008); L. P. Rokhinson, Y. Lyanda Geller, Z. Ge, S. Shen, X. Liu, M. Dobrowolska, and J. K. Furdyna, *ibid.* **76**, 161201 (2007).

⁸A. Richardella, P. Roushan, S. Mack, B. Zhou, D. A. Huse, D. D. Awschalom, and A. Yazdani, *Science* **327**, 665 (2010).

⁹D. Neumaier, M. Turek, U. Wurstbauer, A. Vogl, M. Utz, W. Wegscheider, and D. Weiss, *Phys. Rev. Lett.* **103**, 087203 (2009); Y. Nishitani, D. Chiba, M. Endo, M. Sawicki, F. Matsukura, T. Dietl, and H. Ohno, *Phys. Rev. B* **81**, 045208 (2010); S. Ohya, K. Takata, and M. Tanaka, *Nature Physics* **7**, 342 (2011).

¹⁰K. S. Burch, D. D. Awschalom, and D. N. Basov, *J. Magn. Magn. Mater.* **320**, 3207 (2008).

¹¹G. Acbas, M.-H. Kim, M. Cukr, V. Novak, M. A. Scarpulla, O. D. Dubon, T. Jungwirth, J. Sinova, and J. Cerne, *Phys. Rev. Lett.* **103**, 137201 (2009).

¹²H. Saito, A. Yamamoto, S. Yuasa, and K. Ando, *Appl. Phys. Lett.* **92**, 192512 (2008).

¹³J. G. Braden, J. S. Parker, P. Xiong, S. H. Chun, and N. Samarth, *Phys. Rev. Lett.* **91**, 056602 (2003).

¹⁴C. P. Slichter, *Principles of Magnetic Resonance*, 3rd ed. (Springer, Heidelberg, 1990).

¹⁵V. G. Storchak, D. G. Eshchenko, E. Morenzoni, T. Prokscha, A. Suter, X. Liu, and J. K. Furdyna, *Phys. Rev. Lett.* **101**, 027202 (2008).

¹⁶S. R. Dunsiger, J. P. Carlo, T. Goko, G. Nieuwenhuys, T. Prokscha, A. Suter, E. Morenzoni, D. Chiba, Y. Nishitani, T. Tanikawa, F. Matsukura, H. Ohno, F. Ohe, S. Maekawa, and Y. J. Uemura, *Nat. Mater.* **9**, 299 (2010).

¹⁷M. Sawicki, D. Chiba, A. Korbecka, Y. Nishitani, J. A. Majewski, F. Matsukura, T. Dietl, and H. Ohno, *Nature Physics* **6**, 22 (2010).

¹⁸M. D. Kapetanakis and I. E. Perakis, *Phys. Rev. Lett.* **101**, 097201 (2008).

¹⁹Y. Nojiri, K. Ishiga, T. Onishi, M. Sasaki, F. Ohsumi, T. Kawa, M. Mihara, M. Fukuda, K. Matsuta, and T. Minamisono, *Hyperfine Interact.* **121**, 415 (1999).

²⁰K. Matsuta, M. Sasaki, T. Tsubota, S. Kaminaka, K. Hashimoto, S. Kudo, M. Ogura, K. Arimura, M. Mihara, M. Fukuda, H. Akai, and T. Minamisono, *Hyperfine Interact.* **136**, 379 (2001).

²¹G. Lindner, S. Winter, H. Hofsäss, S. Jahn, S. Blässer, E. Recknagel, and G. Weyer, *Phys. Rev. Lett.* **63**, 179 (1989).

²²K. H. Chow, Z. Salman, W. A. MacFarlane, B. Campbell, T. A. Keeler, R. F. Kiefl, S. R. Kreitzman, C. D. P. Levy, G. D. Morris, T. J. Parolin, S. Daviel, and Z. Yamani, *Physica B* **374-5**, 415 (2006).

²³B. Itermann, G. Welker, F. Kroll, F. Mai, K. Marbach, and D. Peters, *Phys. Rev. B* **59**, 2700 (1999).

²⁴Q. Song *et al.*, *Physica B* **404**, 892 (2009).

²⁵See D. G. Gemmell, *Rev. Mod. Phys.* **46**, 129 (1974), Section 4.2e and references therein; A. E. Michel, R. H. Kastl, S. R. Mader, B. J. Masters, and J. A. Gardner, *Appl. Phys. Lett.* **44**, 404 (1984).

²⁶K. H. Chow *et al.*, *Physica B* **340-2**, 1151 (2003).

²⁷G. D. Morris *et al.*, *Phys. Rev. Lett.* **93**, 157601 (2004).

²⁸E. H. C. P. Sinnecker, G. M. Penello, T. G. Rappoport, M. M. SantaâAnna, D. E. R. Souza, M. P. Pires, J. K. Furdyna, and X. Liu, *Phys. Rev. B* **81**, 245203 (2010).

²⁹Q. Song *et al.*, in Proceedings of the 12th International Conference on Muon Spin Rotation, Relaxation and Resonance, edited by G. M. Luke (submitted to Phys. Proc.).

³⁰K. M. Yu, W. Walukiewicz, T. Wojtowicz, J. Denlinger, M. A. Scarpulla, X. Liu, and J. K. Furdyna, *Appl. Phys. Lett.* **86**, 042102 (2005).

³¹K. M. Yu, W. Walukiewicz, T. Wojtowicz, I. Kuryliszyn, X. Liu, Y. Sasaki, and J. K. Furdyna, *Phys. Rev. B* **65**, 201303 (2002).

³²For example, in contrast to Nb at low temperature, see T. J. Parolin *et al.*, *Phys. Rev. B* **80**, 174109 (2009).

- ³³R. S. Title, *J. Appl. Phys.* **40**, 4902 (1969).
- ³⁴R. E. Walstedt and L. R. Walker, *Phys. Rev. B* **9**, 4857 (1974).
- ³⁵For example, M.-H. Julien *et al.*, *Phys. Rev. B* **63**, 144508 (2001).
- ³⁶R. I. Miller *et al.*, *Physica B* **374**, 30 (2006).
- ³⁷The 150 G $T_1(T)$ measurement in pure GaAs, K. H. Chow *et al.* (unpublished).
- ³⁸For example, M. Shaham, J. Barak, U. El-Hanany, and W. W. Warren Jr., *Phys. Rev. B* **22**, 5400 (1980).
- ³⁹For example, A. Comment, J.-P. Ansermet, C. P. Slichter, H. Rho, C. S. Snow, and S. L. Cooper, *Phys. Rev. B* **72**, 014428 (2005).
- ⁴⁰T. J. Parolin *et al.*, *Phys. Rev. Lett.* **98**, 047601 (2007).
- ⁴¹M. D. Hossain *et al.*, *Physica B* **404**, 914 (2009).
- ⁴²e.g., S. E. Fuller, E. M. Meintjes, and W. W. Warren Jr., *Phys. Rev. Lett.* **76**, 2806 (1996); E. M. Meintjes, J. Danielson, and W. W. Warren Jr., *Phys. Rev. B* **71**, 035114 (2005); M. J. R. Hoch and D. F. Holcomb, *ibid.* **71**, 035115 (2005).
- ⁴³M. Xu *et al.*, *J. Magn. Reson.* **191**, 47 (2008).
- ⁴⁴H. Ohno, A. Shen, F. Matsukura, A. Oiwa, A. Endo, S. Katsumoto, and Y. Iye, *Appl. Phys. Lett.* **69**, 363 (1996).
- ⁴⁵The shift of ^8Li in bulk GaAs relative to ^8Li in MgO at room temperature is less than 10 ppm, Q. Song *et al.* (unpublished).
- ⁴⁶I. Kuryliszyn, T. Wojtowicz, X. Lin, J. K. Furdyna, W. Dobrowolsky, J. M. Broto, O. Portugall, H. Rakota, and B. Raquet, *Acta Phys. Pol. A* **102**, 659 (2002).
- ⁴⁷A. Abragam, *Principles of Nuclear Magnetism* (Oxford University Press, New York, 1983), Chap. VI.
- ⁴⁸T. Jungwirth *et al.*, *Phys. Rev. B* **73**, 165205 (2006).
- ⁴⁹T. J. Parolin *et al.*, *Phys. Rev. B* **77**, 214107 (2008).
- ⁵⁰For example, S. D. Mahanti and T. P. Das, *Phys. Rev. B* **3**, 1599 (1971).
- ⁵¹I. Fan *et al.*, *Physica B* **404**, 906 (2009).
- ⁵²K. Terakura and J. Kanamori, *J. Phys. Soc. Jpn.* **34**, 1520 (1973).
- ⁵³H. Akai, M. Akai, S. Blugel, B. Drittler, H. Ebert, K. Terakura, R. Zeller, and P. H. Dederichs, *Prog. Theor. Phys. Suppl.* **101**, 11 (1990).
- ⁵⁴For example, H. Alloul and P. Bernier, *Ann. Phys. (Paris)* **8**, 169 (1974).
- ⁵⁵B. J. Kirby *et al.*, *Phys. Rev. B* **74**, 245304 (2006).
- ⁵⁶T. R. Beals *et al.*, *Physica B* **326**, 205 (2003).